ISSN: 0067-2904

Detection of Shallow Cavities Using 3D Resistivity Technique in a Small Site Near Haditha City, Western Iraq

Osama H. Al-Jumaily[1*], Kamal K. Ali[1], Jassim M. H. Al Halboosi[2], Ali M. Abed[3]
[1]*Department of Geology, College of Science, Baghdad University, Baghdad, Iraq*
[2]*Department of Geology, College of Science, Baghdad University, Baghdad, Iraq*
[3]*Department of Applied Geology, College of Science, Anbar University, Ramadi, Iraq*

Received: 22/1/2021 Accepted: 23/8/2021 Published: 30/4/2022

Abstract

Iraqi western desert is characterized by a widespread karst phenomenon and caves. Euphrates formation (Lower Miocene) includes enormous sinkholes and cavities within carbonate rocks that usually cause severe damages to any kind of engineering facilities built over it. 3D resistivity imaging techniques were used in detecting this kind of cavities in complicated lithology. The 3D view was fulfilled by collating seven 2D imaging lines. The 2D imaging survey was carried out by Dipole-dipole array with (n) factor and electrode spacing (a) of 6 and 2m respectively. The horizontal slices of the 3D models give a good subsurface picture. There are many caves in all directions (x, y, z). They reveal many small caves near the surface. These caves are clearly shown as points with highly variable resistivity values in slices of depths 0.80 m, 1.72 m, 2.78 m, and 3.99 m. The comparison between standard Least-square and robust constrain methods appeared that the inverse model produced by the robust constrain method has sharper and straighter boundaries. The results of both the two-dimensional and the three-dimensional resistive imaging models deal with almost the same spread of subsurface caves in the study area and show a high amount in number, especially in the upper part, white in color oolitic limestone, the second member of Euphrates Formation, of 3.8-8m depth. 2D and 3D resistivity imaging values have Standard Roof-mean square (RMS) error for large inverted models, this confirms that the study area is of high inhomogeneity. This heterogeneity resulted in a large variation in the resistivity of the rock component in addition to the large spread of caves near the surface.

Keywords: 3D imaging technique, Dipole-dipole array, Karst, Haditha area, Western desert.

الكشف عن الفجوات القريبة من السطح باستخدام تقنية تصوير المقاومة ثلاثية الابعاد في موقع صغير قرب مدينة حديثة غربي العراق

اسامة حمود الجميلي[1*]، كمال كريم علي[1]، جاسم محمد حمد الحلبوسي[2]، علي مشعل عبد[3]
[1*] قسم علوم الارض، كلية العلوم، جامعة بغداد، العراق
[2]قسم علوم الارض، كلية العلوم، جامعة بغداد، العراق
[3] قسم الجيولوجيا التطبيقية، كلية العلوم، جامعة الانبار، العراق

*Email: asamahmood3@gmail.com

الخلاصة

تتميز الصحراء الغربية للعراق بانتشار ظاهرة الكارست والتكهف. يشتمل تكوين الفرات (المايوسين الاسفل) على مجاري ضخمة وبالوعات داخل صخور الكربونات عادة ما تسبب أضرارًا جسيمة لأي نوع من المنشآت الهندسية المبنية فوقها. تقنية التصوير بالمقاومة ثلاثية الأبعاد استخدمت في الكشف عن هذا النوع من التجاويف في الصخر المعقد. تم تحقيق العرض ثلاثي الأبعاد من خلال تجميع سبعة خطوط تصوير ثنائية الأبعاد. تم إجراء المسح التصويري ثنائي الأبعاد بواسطة مجموعة ثنائية القطب مع عامل (ن) وتباعد قطب كهربائي (أ) من 6 و 2 م على التوالي. تعطي الشرائح الأفقية للنماذج ثلاثية الأبعاد صورة جيدة تحت السطح. يوجد العديد من الكهوف في كل الاتجاهات (س ، ص ، ع). يكشف عن وجود العديد من الكهوف الصغيرة بالقرب من السطح. تظهر هذه الكهوف بوضوح كنقاط ذات قيم مقاومة متغيرة للغاية في أقسام من الأعماق 0–0.80 م –1.72 م ، 2.78 م و 3.99 م. اظهرت المقارنة بين طريقتين أن النموذج المعكوس الناتج عن طريقة التقييد القوي له حدود أكثر وضوحًا واستقامة. تتعامل نتائج نموذجي التصوير المقاوم ثنائي الأبعاد وثلاثي الأبعاد تقريبًا مع نفس انتشار الكهوف الجوفية في منطقة الدراسة وتظهر عددًا كبيرًا ، خاصة في الجزء العلوي ، الحجر الجيري ذو اللون الابيض ، والعضو الثاني في تكوين الفرات . تحتوي قيم التصوير بالمقاومة الكهربائية النوعية ثنائية الابعاد وثلاثية الابعاد على خطأ كبير للنماذج المقلوبة. وهذا يؤكد أن منطقة الدراسة ذات عدم تجانس عالٍ. نتج عن عدم التجانس هذا تباين كبير في المقاومة النوعية للمكون الصخري بالإضافة الى الانتشار الكبير للكهوف بالقرب من السطح.

Introduction

The discovery and demarcation of subterranean cavities increased in the last decade, especially with the increase in human activity, development, and the potential collapse and subsidence of near-surface layers leading to problems in human life, civil and environmental engineering. The 2-D and 3-D resistivity imaging technologies, are very useful to characterize the geotechnical site and evaluate subsurface structures such as cavities, voids, and soil stabilization. Several researchers in Iraq used 2-D and 3-D resistivity imaging techniques in engineering applications and environmental studies. Engineering applications included the effect of karst phenomena and gypsum soil on the foundations of buildings and urban facilities. As for the environmental study, it included the pollution of groundwater by oil leaks through fractures in the rocks. [1- 8].

3-D imaging surveys are widely used and give the most accurate results of all geological structures, especially in areas with highly complex or complex geological structures where 2D models are affected by artifacts. However, it cannot reach the same level as surveys in a 2-D way [9- 12]. The main reason is that the scan cost is relatively higher for 3-D imaging for a large area. A complete 3-D resistivity imaging using a 3-D interpretation model should, in theory, give the most accurate results [2]. Real 3-D imaging measurements are collected by placing the electrodes in the form of a 2-D grid and measuring the apparent resistivity along with possible or different directions [13, 14].

The most common strategy or plan for 3-D data measurements is clustering along two-dimensional imaging traverses parallel to possible orthogonal lines. This strategy is more cost-effective and allows each 2-D line to be addressed separately for quality control [15]. Another strategy is to collect data along with several individual directions of the 2-D lines (X or Y), and follow the 2-D reflection to create a 3-D visualization by incorporating these lines into 3D data and a reflection. . In this case, the accuracy of the 3D reflection depends on the spacing between the 2-D lines and the type of electrode array used [15- 17]. In addition, several researchers have described 3D field techniques and they are [18-22].

The main goal of the present study is to delineate the extension of the shallow cavities within the basal breccia unconformity layer between Anah and Euphrates formations and the second member of the Euphrates Formation, which is located near the ground surface.

Materials and methods

Description site and stratigraphy

The study area is located south of Haditha city, western Iraq. It is located between latitude 34° 4'49.66" to 34° 4'44.82"north and longitude 42°21'12.45" to 42°21'46.11" east (Figure 1).

The study area is built up of sedimentary rocks ranging in age from lower Oligocene to Pliocene, with different types of Quaternary deposits (Pleistocene-Holocene). The stratigraphic sequences of geological formations in the area of study as fellows [23]. Shurau and Sheikh Alas formations (Lower Oligocene) are composed of recrystallized limestone (Figure 2). Anah Formation (Lower Oligocene) consists of massive very hard limestone and dolomite limestone. Euphrates formation is the oldest rock outcropped in the studied area. It consists of limestone, dolomite in addition to layers of basal conglomerate [24]. The formation is exposed along both banks of the Euphrates River and in the deep valleys to the south of the Euphrates River. Euphrates Formation is divided into two units: The lower unit consists mainly of conglomerate, gravels followed by layers of limestone that contains fossils; the thickness of this unit ranges from 15-20 meters. The upper unit consists of a sequence of Brescia, limestone, dolomite with horizontal lenses and layers of green shale. The thickness of this unit ranges from 7-15meters [25-27] (Figure 3).

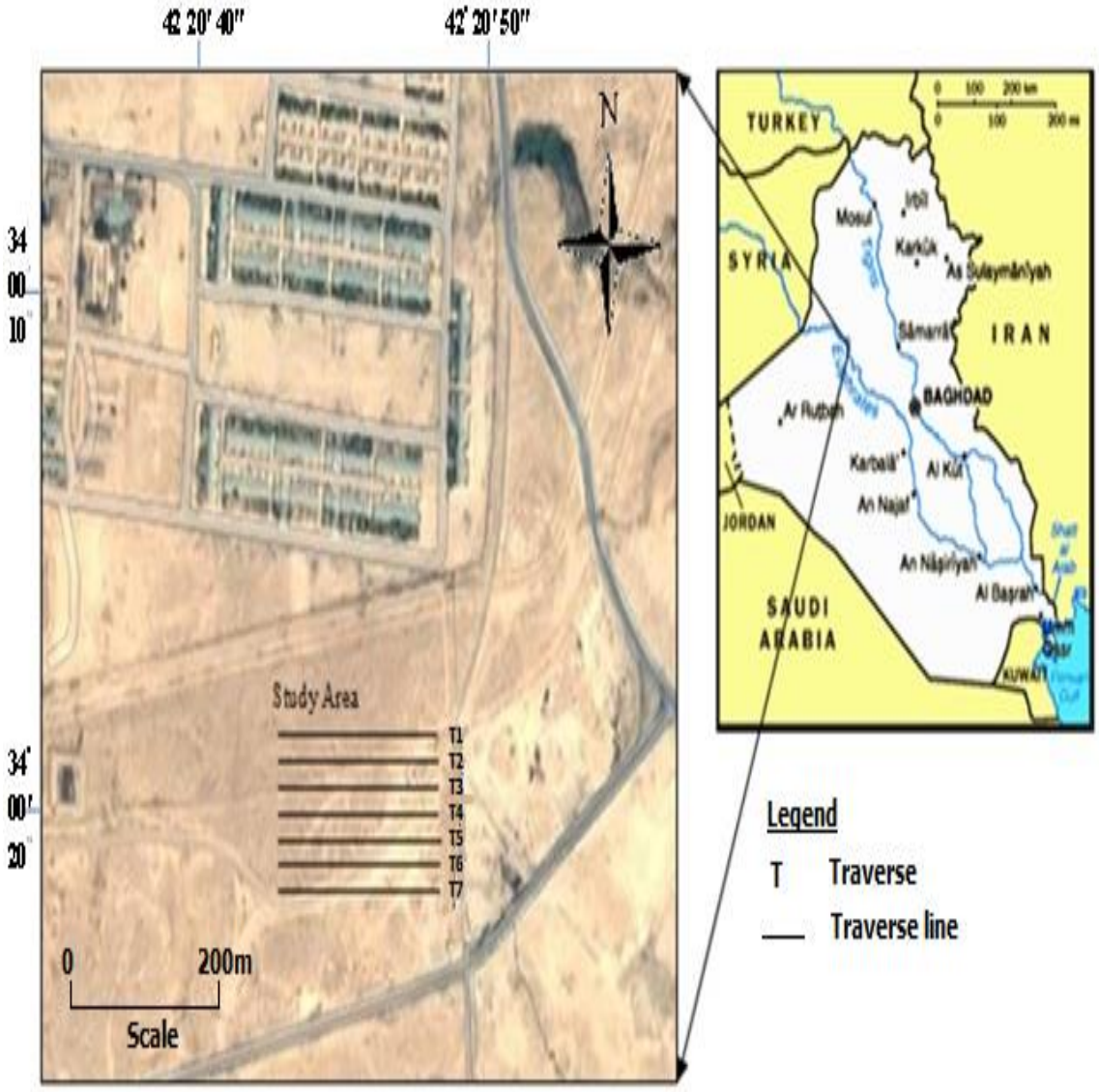

Figure 1- Location map of the study area

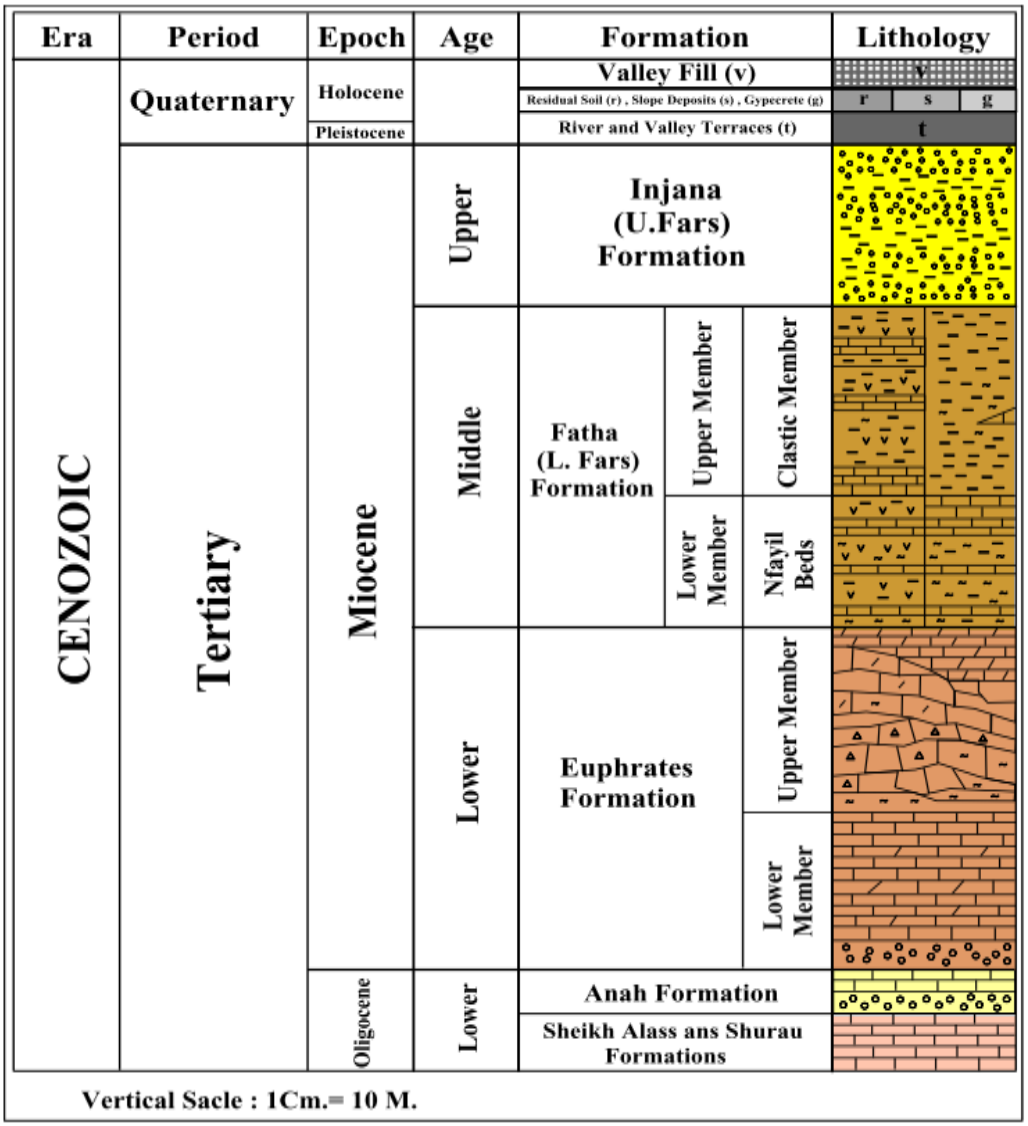

Figure 2- Stratified sequence of geological formations in the studied area [28].

Data Acquisition

The 3D resistivity imaging, with Dipole-dipole array, was performed in the study area with a small area, their dimension 82× 28m. Seven 2-D traverses are carried out of 82 m length and 4 m line distance spacing. The acquisition included dense measurements along these seven parallel lines in a west-east direction to achieve a 3-D image. Possible instead of a 2-D grid or vertical 2-D lines to shoot in the X and Y directions takes more time, effort, and cost. Resolution of the 3-D image obtained from subsurface dense measurements. The two-dimensional parallel lines were merged to form a 3D imaging that represents the real and sterile image of the caves below the surface [11,18, 29].

In this study, seven parallel survey lines (T1, T2, T3------- T7) where, all the survey lines above a selected area chosen near the K3- cavity, which occurred as a result of a bulldozer working to level the land to build a primary school. The Terrameter SAS 4000 instrument was used for measuring 2-D resistivity data.

3-D display of subsurface structural geology data files for a small area within the study area (seven profiles), mapped into a single data file that can be read using the RES3DINV software which tends to be inverted. RES3DINV is a computer software [30] that will automatically

determine a 3-D resistivity model below the surface using data obtained from a 3-D electrophoresis image[31, 32].

The inversion routine used by the software is based on the smoothly constrained least-squares method [31]. A new application of the least-squares method based on Newton's quasi-refinement technique can also be used [30]. This technique can be 10 times faster than the traditional least-square method for large data sets and requires less memory. One advantage of this method is that the damping factor and flatness filters can be adjusted to suit different types of data.

In this software, we can also use the traditional Gauss-Newton method which recalculates the Jacobian matrix of partial derivatives after each iteration [31]. It is much slower than the quasi-Newton method, but in areas with large resistivity contrasts greater than 10:1, it gives slight results. The third option in this software is to use the Gauss-Newton method for the first 2 or 3 iterations, after which the quasi-Newton method is used. In many cases, this provides the best compromise.

Results and Discussion

The software can display inversion results as slices with different depths, the depth to every slice can be set by the user. Every slice represents a map of true resistivity distribution within the chosen depth.

Figure 3 shows a very good 3D distribution of true resistivity in the x and y direction with depth. First and second slices which are represented the resistivity from the surface to (2m) depth show relatively higher resistivity reflecting the dry sediments.

The horizontal sections of the 3D models give a good picture. There are many cavities in all directions (x, y, z). It reveals the presence of many small caves near the surface. These cavities are clearly shown as points with highly variable resistivity values in sections of depths 0.80 m, 1.72 m, 2.78 m, and 3.99 m, to reflect the heterogeneity between the rock components in this zone.

The first three slices, which reach a depth of 6.13 m, indicate a high rise in the resistivity values this is the result of the dry of exposed surface layers with some small shallow cavities formed as a result of rainwater infiltration. The fourth, fifth, and sixth slices, such as a number of cavities located between depths 6.13 to 11.8 m, show a large spread of cavities. Someplace with low values of resistivity such as 0.5 to 2.3 ohm.m, confirms the presence of the water leaking from rain and groundwater. While the seventh to twelfth slices and extending between the depth of 11.5 to 20.3 m, the number of the cavities decreases with a decrease in resistivity values. this indicates that the region is characterized by a shallow cavity, while is more dangerous for engineering projects. This is consistent with the studies conducted by [2, 8, 9, 25, 31] to study the karst phenomena of the areas adjacent to the study area, in terms of the spread and size of caves.

From the inverse models in (Figure 3) and (Figure 4). The comparison between the two methods appeared that the inverse model produced by the robust constrain method (Figure 4) has sharper and straighter boundaries.

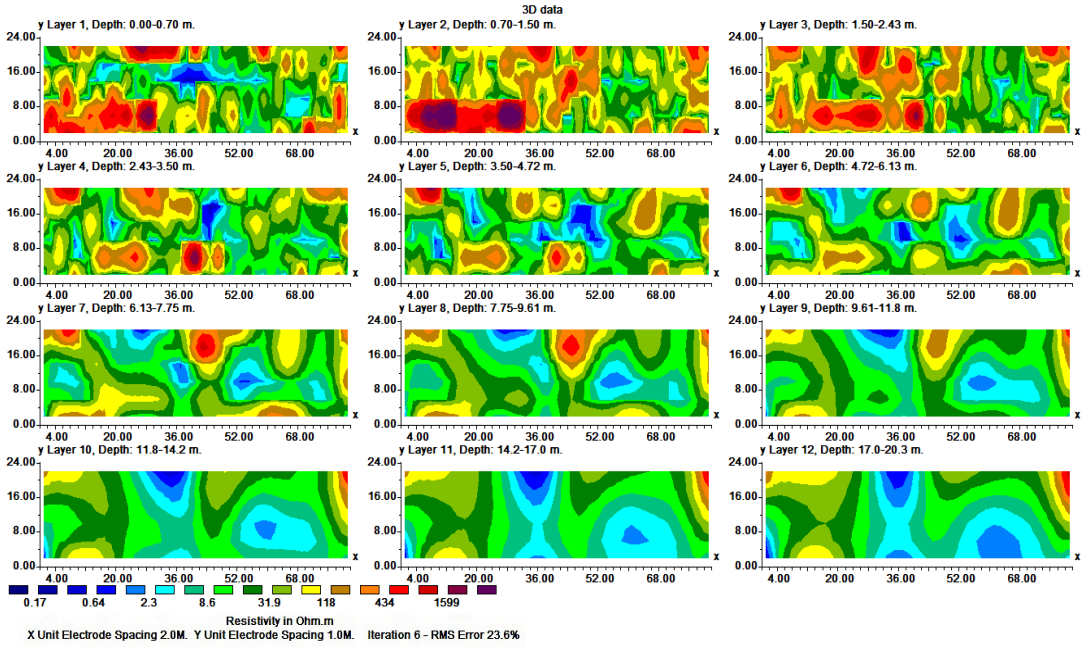

Figure 3- Inversion model for shallow unknown cavities shows horizontal slices of the 3D resistivity distribution with depth using standard Least-square method

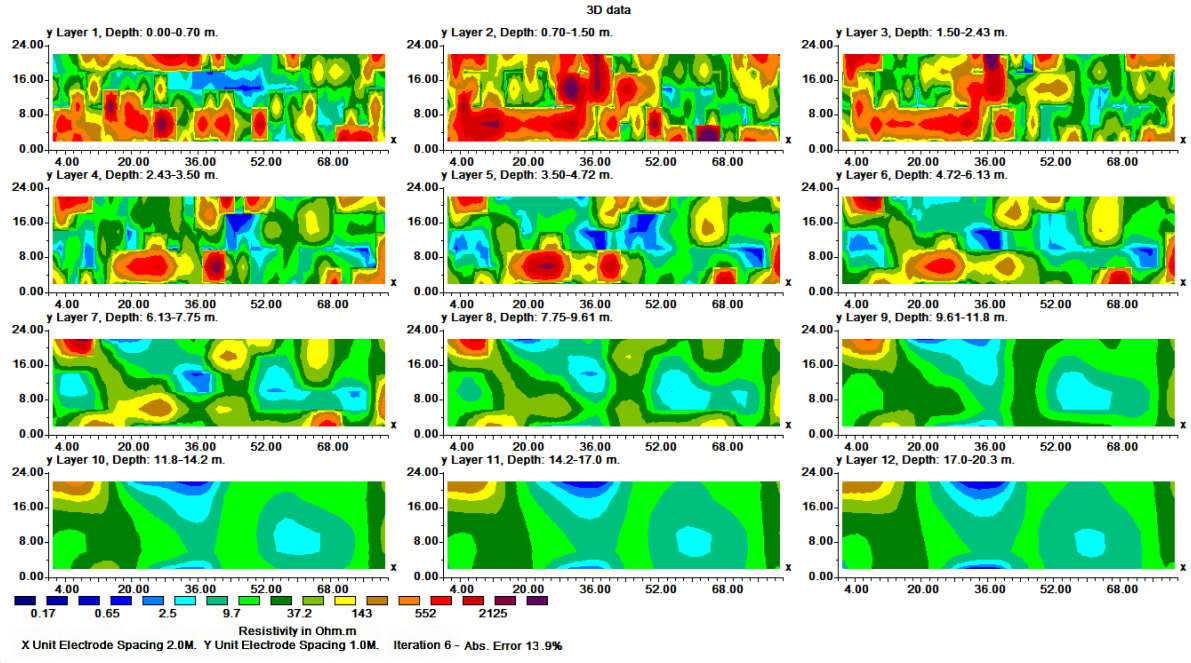

.

Figure 4- Inversion model for shallow unknown cavities shows horizontal slices of the 3D resistivity distribution with depth using robust constrain method.

The results of both the two-dimensional and the three-dimensional resistive imaging models deal with almost the same spread of subsurface caves in the study area and show a high amount in number, especially in the upper part, the unconformity between the Anah and Euphrates formations.

Each of the 2-D and 3-D resistivity imaging values shows RMS error for large models Inverted, this indicates that the probe area is characterized by high inhomogeneity. This heterogeneity resulted in a large variation in the resistance of the rock component in addition to the large spread of caves near the surface. These results indicate that the area represents a risky environment for the buildings constructed in it or planned for future construction.

Conclusions

The horizontal slices of the 3D models give a good picture. There are many caves in all directions (x, y, z). It reveals the presence of many small caves near the surface. These caves are clearly shown as points with highly variable resistivity values in sections of depths 0-0.80 m, 0.80-1.72 m, 1.72-2.78 m, and 2.78-3.99 m. The comparison between standard Least-square and robust constrain methods appeared that the inverse model produced by the robust constrain method has sharper and straighter boundaries. The results of both the 2D and the 3D resistivity imaging models deal with almost the same spread of subsurface caves in the study area and show a high amount in number, especially in the upper part, white in color oolitic limestone, a second member of Euphrates Formation. 2D and 3D resistivity imaging values have an RMS error for large inverted models, this confirms that the probe area is of high homogeneity. This heterogeneity resulted in a large variation in the resistivity of the rock component in addition to the large spread of caves near the surface. These results indicate that the area represents a risky environment for the buildings constructed in it or planned for future construction.

Acknowledgments

The authors thanked the Head and members of the Department of Applied Geology in the college of science, the University of Anbar for their important geological information when conducting this research. Likewise, they would like to thank the Dean of the College of Science (Anbar University) for providing them with SAS-4000 devices, electrodes, electrode cables, etc., which were necessary for conducting the field survey.

References

[1] M. Mohamed, A.K. Mohamed, Al-Sayed, El-Said, El-Kenawy Abeer. 2012. Tracing subsurface oil pollution leakage using 2D electrical resistivity tomography. Arab J Geosci 6(9):3527–3533

[2] J. M. Thabit, A. M. Abed, 2014. Detection of subsurface cavities by using pole- dipole array (Bristow's method)/hit area-western Iraq, Iraqi Journal of Science, 55: 444–453.

[3] H. Abdelwahab, 2013. Comparison of 2D and 3D Resistivity Imaging Methods in the Study of Shallow Subsurface Structures. Greener Journal of Physical Sciences, 3(4): 149-158.

[4] A. A. Hassan, and Naif, M. D., 2016. Application of 2D electrical resistivity imaging technique for detecting soil cracks: Laboratory study. Iraqi Journal of Science, 57: 930–937.

[5] A.A. Amini and H. Ramazi, 2017. CRSP, numerical results for an electrical resistivity array to detect underground cavities. Open Geosciences, 9: 13–23. https://doi.org/10.1515/geo-2017-0002.

[6] N. A. Aziz, Z. T. Abdulrazzaq and O. E. Agbasi, 2019. Mapping of subsurface contamination zone using 3D electrical resistivity imaging in Hilla city, Iraq. Environmental Earth Sciences, 78: 502. https://doi.org/10.1007/s12665-019-8520-9.

[7] A. M Salman, A. M Abed and J. M. Thabit, 2020. Comparison between Dipole-dipole and Pole-dipole arrays in delineation of subsurface weak zones using 2D electrical imaging technique in Al-Anbar University, Western Iraq, Iraqi Journal of Science, 61 (3): 567-576.

[8] A. M Salman, J. M. Thabit, A. M. Abed, 2020. Application of the electrical resistivity method for site Investigation in the University of Anbar, Ramadi City, Western Iraq, Iraqi Journal of Science, 61(6): 1345-1352.

[9] M.H. Loke, J.E. Chambers, D.F. Rucker, O. Kuras and P.B. Wilkinson, 2013. Recent developments in the direct-current geoelectrical imaging method. J Appl Geophys 95:135–156

[10] T. Dahlin and M.H. Loke, 1997. Quasi-3D resistivity imaging: mapping of 3D structures using two-dimensional dc resistivity techniques, 3rd Mtg., Environ. Eng. Geophysics. Assn., Expanded Abstracts, pp 143–146.

[11] T. Dahlin, C. Bernstone and M.H. Loke, 2002. A 3-D resistivity investigation of a contaminated site at Lernacken, Sweden. Geophysics 67(6):1692–1700.

[12] L.R. Bentley, M. Gharibi, 2004. Two- and three-dimensional electrical resistivity imaging at a heterogeneous remediation site. Geophysics 69:674–680

[13] J.E. Chambers, O. Kuras, P.I. Meldrum, R.D. Ogilvy and J. Hollands, 2006. Electrical resistivity tomography applied to geologic, hydrogeologic, and engineering investigations at a former waste-disposal site. Geophysics 71(6): B231–B239.

[14] J.E. Chambers, P.B. Wilkinson, D. Wardrop, A. Hameed, I. Hill, C. Jeffrey, M.H. Loke, P.I. Meldrum, O. Kuras, M. Cave, and D.A Gunn, 2012. Bedrock detection beneath river terrace deposits using three-dimensional electrical resistivity tomography. Geomorphology 177–178:17–2520.

[15] D.F. Rucker, M.T. Levitt, and W.J. Greenwood, 2009. Three-dimensional electrical resistivity model of a nuclear waste disposal site. J Appl Geophys 69(3–4):150–164.

[16] T., Dahlin and M.H. Loke, 1997. Quasi-3D resistivity imaging: mapping of 3D structures using two-dimensional dc resistivity techniques, 3rd Mtg., Environ. Eng. Geophysics. Assn., Expanded Abstracts, pp 143–146.

[17] X. Yang and N. Lagmanson, 2006. Comparison of 2D and 3D electrical resistivity imaging methods. SAGEEP proceedings, pp 585–594.

[18] M.H. Loke, 2020. Tutorial: 2D and 3D electrical imaging surveys. 188p.

[19] M.H. Loke and R.D. Barker, 1996. Practical techniques for 3D resistivity surveys and data inversion. Geophys Prospect 44:499–524.

[20] R.M.S. White, S. Collins, R. Denne, R. Hee and P. Brown, 2001. A new survey design for 3D IP modeling at Copper hill. Explore Geophys 32(4):152–155.

[21] T. Dahlin, C. Bernstone and M.H. Loke, 2002. A 3-D resistivity investigation of a contaminated site at Lernacken, Sweden. Geophysics 67(6):1692–1700.

[22] M.H. Loke and T. Dahlin, 2010. Methods to reduce banding effects in 3-D resistivity inversion. In: Proceedings of the 16th European Meeting of Environmental and Engineering Geophysics, 6–8 Sep 2010, Zurich, Switzerland, A16.

[23] A. M. Abed, A. S. Al-Zubedi, and Z. T. Abdulrazzaq, 2020. Detected of gypsum soil layer by using 2D and 3D electrical resistivity imaging techniques in University of Anbar, Iraq, Iraqi Geological Journal, 53 (2C):134-144.

[24] V. Sissakian, E. F. Ibrahim and N. AL-Ali, 2005.Explanatory of Geological Hazard Map of Iraq 1st Edition, (Scale 1:1000000) D. Geol. Surv. (GEOSURV) Min. Invest, Baghdad.

[25] M. F. T. Al -Ghreri, 2007. Bio stratigraphic succession of the formations in the upper Euphrates valley in the area between Hit and Al-Qaim. PH thesis, geology department, science college, Baghdad.

[26] S. Z. Jassim and J. C. Goff, (edts)., 2006. Geology of Iraq. Published by Dolin, Prague and Moravian Museum, Berno, 341pp.

[27] T. Gunther, C. Rucker and K Spitzer, 2006. Three-dimensional modeling and inversion of dc resistivity data incorporating topography— II. Inversion. Geophys J Int 166:506–517.

[28] M. F. T. Al-Ghreri, 2007. Bio stratigraphic succession of the formations in the upper Euphrates valley in the area between Hit and Al-Qaim. PH thesis, geology department, science college, Baghdad.

[29] Geotomo Software. RES2DINVx64 user manual ver. 4.09 with multi-core and 64-bit support, Geoelectrical Imaging 2-D and 3-D. Geotomo Software Sdn, Bhd. 2019; http://www.geotomosoft.com/.

[30] A.S. Al-Zubedi and J.M. Thabit, 2015. Use of 2D azimuthal resistivity imaging in delineation of the fracture characteristics in Dammam aquifer within and out of Abu-Jir fault zone, central Iraq, Arab J Geosci.; 8:1–9.

[31] O. J. Mohammed, A. M. Abed and M. A. Alnuaimi, 2021. Evaluation and Delineation of Sulfur Groundwater Leakages Using Electrical Resistivity Techniques in Hit Area, Western Iraq. Iraqi Journal of Science, 2239-2249.

[32] F. A. Obaid, A. M. Al-Rahim and H. Z. Ali, 2020. Subsurface Imaging of 2D Seismic Data Using Kirchhoff Time Migration Method, Central Iraq. Iraqi Journal of Science, 3318-3326.